

Fig. 3 shows the high pressure DTA curve of  $\text{MmCo}_5\text{-H}$  system when the  $\text{MmCo}_5\text{H}_{2.5}$  was heated at  $10^6$  Pa of hydrogen, the curve had three endothermic peaks. It is assumed that these peaks correspond to the dissociations of three hydrides respectively, whose composition and crystal structures are each slightly different.

The composition of hydride at  $25^\circ\text{C}$  under  $10^6$  Pa, the desorption pressure of hydride

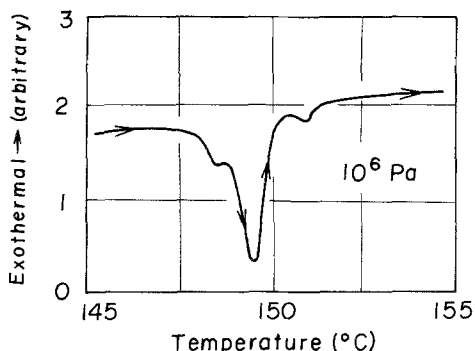


Figure 3 High pressure DTA curve for dissociation of hydride in  $\text{MmCo}_5\text{-H}$  system.

$\text{MmCo}_5\text{H}_{1.25}$  at  $25^\circ\text{C}$ , and the enthalpy change for the dissociation of hydride, calculated using the values for  $\text{CeCo}_5\text{-H}$ ,  $\text{LaCo}_5\text{-H}$ ,  $\text{PrCo}_5\text{-H}$  and  $\text{NdCo}_5\text{-H}$  systems measured by Kuijpers [1], are  $\text{MmCo}_5\text{H}_{2.5}$ ,  $1.2 \times 10^5$  Pa, and 0.42 eV, respectively. The composition of the hydride at  $25^\circ\text{C}$  under  $10^6$  Pa, and the desorption pressure ( $1.1 \times 10^5$  Pa) of  $\text{MmCo}_5\text{H}_{1.25}$  at  $25^\circ\text{C}$  in this work were in good agreement with the calculated values, but the enthalpy change for the dissociation of hydride was smaller than the calculated one. This difference may be due to the effects of element alloying.

## References

1. F. A. KUIJPERS, Philips Research Report Supplement, (1973) No. 2.
2. H. H. VAN MAL, *ibid* (1976) No. 1.
3. M. KITADA, *J. Japan. Inst. Metals*, **41** (1977) 420.

Received 18 February  
and accepted 11 March 1977.

MASAHIRO KITADA,  
Central Research Laboratory,  
Hitachi Ltd., Tokyo, 185,  
Japan

## Factors affecting the stress dependence of creep of polycrystalline ceramics

Under high temperature creep conditions, the variation of the secondary or steady-state creep rate,  $\dot{\epsilon}_s$ , with stress,  $\sigma$ , at a constant temperature,  $T$ , can be expressed in the form

$$\dot{\epsilon}_s|_T \propto \sigma^n$$

With many polycrystalline ceramics, the stress exponent  $n$  is found to decrease from values of 3 or more, at high stresses, to values approaching unity at low stress levels. With this type of material, deformation at high stresses is considered to occur by the generation and movement of dislocations whilst, in the low-stress range, creep is usually attributed to stress-directed vacancy diffusion. It has been suggested that polycrystalline ceramics showing this type of behaviour can be classified into two groups, depending on the  $n$  value generally reported for creep in the high-stress range [1]. One group exhibits a stress exponent of approximately 5 (e.g. NaCl, LiF, CaO,

$\text{UO}_2$ ) whilst the other group displays an  $n$  value close to 3 (e.g. MgO, BeO,  $\text{Al}_2\text{O}_3$ ). This difference in stress exponent is not simply a consequence of differences in the nature of the atomic bonds (2) since, for example, CaO and MgO both have a rock salt structure and similar bond-type, but display different  $n$  values at high stress levels (Fig. 1). Alternatively, the results presented in Fig. 1 are compatible with a classification [1] which links the  $n$  value to the ratio of the radii of the anion  $r_a$  and the cation  $r_c$ , with  $n \approx 5$  for materials with  $r_a/r_c < 2$ , and  $n \approx 3$  for ceramics with  $r_a/r_c > 2$ . However, evidence is available which indicates that a specific  $n$  value of 3 or 5 should not be assigned to each ceramic material. In particular, for polycrystalline MgO samples of similar purity, porosity and grain size, the  $n$  value has been shown to vary in the range  $\sim 2$  to  $\sim 7$  depending on the fabrication procedures used to prepare the testpieces [5]. The present work aims to rationalize the conflicting observations on stress exponents in terms of the slip behaviour of ceramic materials, a view consistent with the known

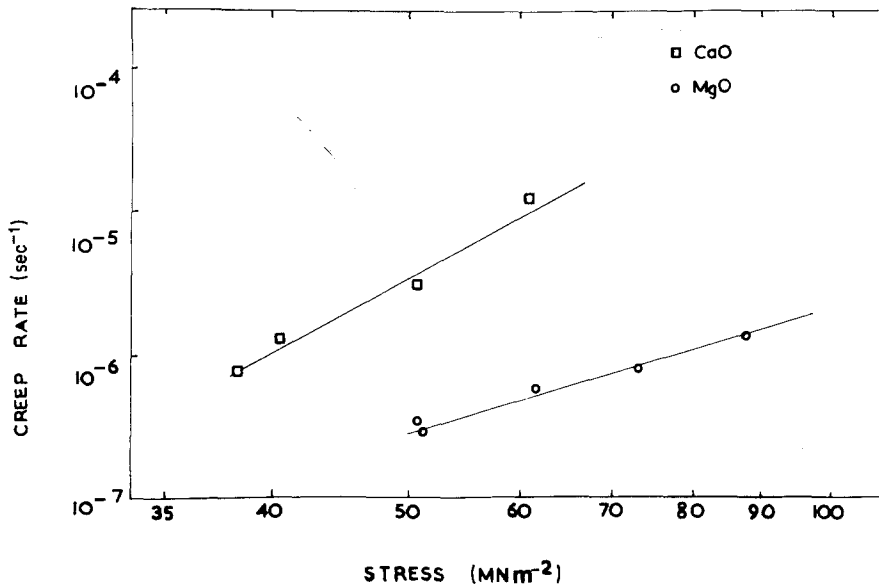


Figure 1 The dependence of the steady-state creep rate,  $\dot{\epsilon}_s$ , on the applied stress,  $\sigma$ , for polycrystalline lime at 1473 K [3] and for polycrystalline magnesia at 1596 K [4].

importance of slip processes during creep of polycrystalline ceramics at high stress levels.

For MgO and CaO, slip occurs in  $\langle 1\bar{1}0 \rangle$  directions on  $\{110\}$  planes, with slip also possible on  $\{001\}$  planes. At room temperature, for both lime and magnesia, the resolved shear stress required for slip on  $\{001\}$  planes is much greater than that needed for slip on  $\{110\}$  planes. With increasing temperature, the ratio of the stress to initiate slip on  $\{001\}$  planes to that for slip on  $\{110\}$  planes decreases. In order to satisfy the von Mises criterion that five independent slip systems must operate to achieve homogeneous plastic deformation of a polycrystal, slip must

occur at similar stress levels on both  $\{001\}$  and  $\{110\}$  planes in MgO and CaO [6]. This requirement is satisfied for lime at  $\sim 1250$  K [7] whereas temperatures in excess of  $\sim 2000$  K are necessary with magnesia [8]. Thus, at the creep temperatures examined (Fig. 1), an  $n$  value of  $\sim 5$  was found for the highly ductile lime [3], compared with a value of  $\sim 3$  for the magnesia which exhibited more limited ductility [4].

The temperature of the brittle-ductile transition for a number of polycrystalline ceramics is shown in Table I, which also includes the temperature range over which the stress exponent for creep was determined. It appears that  $n \approx 5$  for

TABLE 1 The temperature of brittle-ductile transition in relation to the stress exponent for creep at elevated temperature of polycrystalline ceramics.

Material	Temperature of brittle-ductile transition (K)	Reference	Stress exponent $n$ at high stresses	Creep temperature (K)	Reference
NaCl	$\sim 470$	[6, 9, 16]	5	$\sim 700-900$	[13]
KCl	$\sim 520$	[15]	5	$\sim 900$	[13]
LiF	$\sim 620$	[17]	6.6	$> \sim 670$	[18]
UO <sub>2</sub>	$\sim 1420$	[11]	5	$> 1470$	[19]
UC	$\sim 1270-1470$	[20]	5	1470-1970	[20]
CaO	$\sim 1250$	[7]	5	1470	[3]
MgO	$\sim 2000$	[11]	3	1600	[4]
BeO	-	[9, 21]	3	$\sim 2100$	[22]
Al <sub>2</sub> O <sub>3</sub>	-	[11]	3	$\sim 1800-2000$	[23]
MgAl <sub>2</sub> O <sub>4</sub>	-	[9]	3	$\sim 1800$	[24]

materials exhibiting ductile behaviour. In this way, the correlation noted [1] between the  $n$  value at high stresses and the ratio  $r_a/r_c$  can be accounted for since the radius ratio is related to the polarizability, and hence the slip characteristics, of ionic solids. In general, ductile behaviour requires the operation of 5 independent slip systems. However, with spinel, although 5 slip systems operate even at room temperature, the lack of interpenetration of the slip systems limits ductility [9], compatible with an  $n$  value of 3 being recorded. Conversely, with  $\text{UO}_2$ , slip appears to take place at similar stress levels on  $\{001\}$  and  $\{110\}$  planes only at temperatures above  $\sim 2150\text{K}$  [10]. Yet, the occurrence of cross slip results in ductile behaviour of  $\text{UO}_2$  above  $\sim 1470\text{K}$  [11], in agreement with  $n \simeq 5$ .

A dependence of  $n$  value on the ductility of polycrystalline ceramics would also be in agreement with known variation of  $n$  with fabrication procedure for  $\text{MgO}$  [5]. Several studies using polycrystalline  $\text{MgO}$  have shown that minor differences in pore size and distribution, composition and grain size arising as a consequence of different specimen fabrication techniques can result in significant variations in mechanical properties, and especially in the temperature representing the onset of general ductility [12]. It has been proposed that differences in plasticity depend on whether the grain boundaries are sufficiently strong to allow stress concentrations to build up to initiate slip on  $\{001\}\langle 1\bar{1}0\rangle$  systems [12]. The high temperature ductility, and hence the stress exponent for creep, therefore depends on the detailed microstructure of the material and consequently on the sample preparation methods.

It then appears that, for nominally-pure polycrystalline ceramics,  $n$  values of  $\sim 5$  are obtained at high stress levels with materials displaying ductile behaviour at the creep temperature, whereas lower  $n$  values are associated with brittle or semi-brittle behaviour. Exceptions to this correlation may, however, be found for creep of solid solutions. Pure  $\text{KCl}$  and  $\text{NaCl}$  are ductile at creep temperature examined, compatible with the reported  $n$  values of  $\sim 5$  (Table I). Yet,  $\text{KCl}$ – $\text{NaCl}$  solid solutions display  $n$  values of  $\sim 3$  [13]. As suggested by Cannon and Sherby [13], this may well represent behaviour typical of dislocation movement controlled by solute drag [14]. Even

so, an alternative interpretation may be possible, based on the slip behaviour of solid solutions. Although no information appears to be available on the deformation characteristics of the  $\text{KCl}$ – $\text{NaCl}$  system, work has been undertaken on  $\text{KCl}$ – $\text{KBr}$  solid solutions [15]. The temperature at which slip occurs at similar stress levels on  $\{110\}$  and  $\{001\}$  planes is raised from  $\sim 500\text{K}$  for pure  $\text{KCl}$  to  $\sim 800\text{K}$  for a  $\text{KCl}$ –19%  $\text{KBr}$  solid solution. The occurrence of  $n$  values of  $\sim 3$  for  $\text{KCl}$ – $\text{NaCl}$  solid solutions may then represent either solute-drag control of dislocation movement during creep, or behaviour comparable with that for nominally-pure materials of limited ductility.

### Acknowledgements

One of the authors (B. Watkins) is indebted to the Science Research Council for a maintenance grant during the period of this research.

### References

1. W. R. CANNON and O. D. SHERBY, *J. Amer. Ceram. Soc.* **56** (1973) 157.
2. S. H. KIRBY and C. B. RALEIGH, *Tectonophysics* **19** (1973) 165.
3. J. A. COATH and B. WILSHIRE, *Ceramurgia Int.* (1977) to be published.
4. J. M. BIRCH and B. WILSHIRE, *J. Mater. Sci.* **9** (1974) 794.
5. P. C. DOKKO. and J. A. PASK, *Mat. Sci. Eng.* **25** (1976) 77.
6. G. W. GROVES and A. KELLY, *Phil. Mag.* **8** (1963) 877.
7. C. HULSE and J. BATT, Office of Naval Res. Rep. (U S) May 1974. Contract No. N0014-69-C-0073. Project No. NR032-516/9-28-72.
8. S. M. COPLEY and J. A. PASK, *J. Amer. Ceram. Soc.* **48** (1965) 139.
9. K. C. RADFORD and G. R. TERWILLIGER, *Bull. Amer. Ceram. Soc.* **53** (1974) 172.
10. E. J. RAPPERPORT and A. M. HUNTRESS, *Nuclear Metals Inc.*, Rep. No. NMI 1242 (1960).
11. A. G. EVANS and R. W. DAVIDGE, *Mat. Sci. Eng.* **6** (1970) 281.
12. A. G. EVANS and T. G. LANGDON, *Prog. Mater. Sci.* **21** (1976) 171.
13. W. R. CANNON and O. D. SHERBY, *J. Amer. Ceram. Soc.* **53** (1970) 346.
14. J. WEERTMAN, *J. Appl. Phys.* **28** (1957) 1185.
15. N. S. STOLLOFF, D. K. LEZIUS and T. L. JOHNSTON, *ibid* **34** (1963) 3315.
16. R. J. STOKES, *Proc. Brit. Ceram. Soc.* **6** (1966) 189.
17. D. W. BUDWORTH and J. A. PASK, *Trans. Brit. Ceram. Soc.* **62** (1963) 767.
18. D. R. CROPPER and T. G. LANGDON, *Phil. Mag.* **18** (1968) 1181.

19. L. E. POTEAT, and C. S. YUST, "Ceramic Microstructures" (Wiley, New York, 1968) p.646.
20. J. L. ROUTBORT and R. N. SINGH, *J. Nucl. Mat.* **58** (1975) 78.
21. G. G. BENTLE and K. T. MILLER, *J. Appl. Phys.* **38** (1967) 4248.
22. W. L. BARMORE and R. R. VANDERVOORT *J. Amer. Ceram. Soc.* **50** (1967) 316.
23. S. I. WARSHAW and F. H. NORTON, *ibid* **45** (1962) 479.
24. H. PALMOUR III, *Proc. Brit. Ceram. Soc.* **6** (1966) 209.

Received 21 February  
and accepted 11 March 1977

B. WILSHIRE,  
B. WATKINS,  
*Department of Metallurgy and  
Materials Technology  
University College,  
Singleton Park,  
Swansea, U K*

### *Microstructural changes during the argon-sintering of silicon powder compacts*

Reaction-bonded silicon nitride (RBSN) is gaining acceptance as an engineering ceramic, and attention is being focused on how processing affects its microstructure [1, 2]. This is because both mechanical properties and oxidation resistance are microstructure-dependent and require optimizing if the material is to be successfully exploited in high temperature engineering.

The fabrication route for RBSN involves the following three main stages: (i) production of the silicon powder compact when particle size, size distribution and the compaction operation are important; (ii) argon-sintering (typically at  $\sim 1200^\circ\text{C}$ ), in which the compact gains sufficient strength to withstand the machining stresses, and (iii) nitriding, during which conversion to the ceramic occurs.

Current Leeds research is concerned with examining the extent to which each stage determines final microstructure. As far as stage (iii) is concerned, the situation is complicated, because the reaction is very sensitive to impurities [3] which are invariably present in significant amounts in the production of commercial material. A firm basis is being established for the control of microstructure during nitriding [4]; the present letter draws attention to some important features of the microstructure developed during argon-sintering, the stage which, as far as the authors are aware, has received little or no attention hitherto.

To investigate the changes in microstructure occurring during this stage, a commercial silicon powder (conventionally ground in a steel ball-mill; analysis in Table I) was isostatically pressed at  $200\text{ MN m}^{-2}$  into compacts which were argon-sintered at 1150, 1200 or  $1250^\circ\text{C}$  for 1 or 18 h.

TABLE I Analysis of silicon powders

Sample	Composition (Wt %)		
	Ca	Al	Fe
Commercially ground Si (powder 1)	0.20	0.24	0.96
Ceramic ground Si (powder 2)	0.10	1.0	0.31

Chemical analysis at points within the compacts was estimated using the energy dispersive Link System attachment to a Cambridge S600 scanning microscope. Fig. 1a shows the microstructure of a compact before argon-sintering; Fig. 1b is typical of the microstructure developed during argon-sintering.

In a comparison experiment, lump silicon (from the same source as that of Powder 1) was ground in a ceramic mill, to avoid metallic iron contamination (analysis in Table I). The microstructure of a compact of this powder, after sintering in argon at  $1250^\circ\text{C}$  for 18 h, is shown in Fig. 1c.

The large voids in Fig. 1b, which were a common feature of these particular samples, were evidently caused by local melting, followed by movement of the melt, due to surface tension forces, into adjacent regions. Each pore had a second phase associated with it, clearly shown up by relief-polishing (Fig. 1d). The composition by weight of this phase was estimated by probe analysis to be Si (51%), Fe (47%) and Al (1.5%). A point by point analysis along a line through the pore confirmed that the iron-rich melt had in fact moved into the surrounding compact (Fig. 2).

The composition of the melt is close to that of the eutectic  $\text{FeSi}_2$  [5], having melting point  $1212^\circ\text{C}$ . The extent of second phase associated with a pore increased with increasing temperature and its average composition followed the liquidus in the silicon-rich direction. It seems likely that aluminium could account for the melting observed at  $1150^\circ\text{C}$ , but this requires confirmation.